

GRAPHENE OXIDE-LOADED SHORTENING AS AN ENVIRONMENTALLY FRIENDLY HEAT TRANSFER FLUID WITH HIGH THERMAL CONDUCTIVITY

by

**Thammasit VONGSETSKUL^{a*}, Peeranut PRAKULPAWONG^a,
Panmanas SIRISOMBOON^b, Jonggol TANTIRUNGROTECHAI^a,
Chanasuk SURASIT^a, and Pramuan TANGBORIBOONRAT^a**

^aDepartment of Chemistry, Faculty of Science, Mahidol University, Ratchathewi, Bangkok, Thailand

^bDepartment of Mechanical Engineering, Faculty of Engineering,
King Mongkut's Institute of Technology Ladkrabang, Bangkok, Thailand

Original scientific paper

<https://doi.org/10.2298/TSCI150312199V>

Graphene oxide-loaded shortening (GOS), an environmentally friendly heat transfer fluid with high thermal conductivity, was successfully prepared by mixing graphene oxide (GO) with a shortening. Scanning electron microscopy revealed that GO particles, prepared by the modified Hummer's method, dispersed well in the shortening. In addition, the latent heat of GOS decreased while their viscosity and thermal conductivity increased with increasing the amount of loaded GO. The thermal conductivity of the GOS with 4% GO was higher than that of pure shortening of ca. three times, from 0.1751 to 0.6022 W/mK, and increased with increasing temperature. The GOS started to be degraded at ca. 360 °C. After being heated and cooled at 100 °C for 100 cycles, its viscosity slightly decreased and no chemical degradation was observed. Therefore, the prepared GOS is potentially used as environmentally friendly heat transfer fluid at high temperature.

Key words: heat transfer fluid, GO, shortening, thermal conductivity

Introduction

Heat transfer fluid (HTF) is a liquid substance used to carry heat away from its source to be cooled. It is used to monitor heat and temperature [1] and determine the efficiency of heat utilization in various applications such as chemical processing, concentrated solar power, food and beverage processing, pharmaceutical and plastic processing, and system maintenance. In solar thermal energy, the solar collectors convert solar radiation into heat that transfers through HTF to a heat exchanger [2]. This heat boils water and produces steam. Since the electricity is obtained from turbine driven by steam, it is directly proportional to the amount of heat transferred to water.

Based on the operation temperatures, HTF can be classified as low and high temperature ones. Water based liquid containing alcohol or diol is low temperature HTF whereas petroleum based and synthetic mineral oils such as silicone and paraffinic oil, alkylated aromatic, and fluorocarbon are used at high operating temperature. However, these high temperature HTF are not biodegradable and not derived from renewable resources. Thus, shortening, a mixture of fatty acid and triglycerides of vegetable origin, is introduced for environmental-friendly reason.

*Corresponding author, e-mail: thammasit.von@mahidol.ac.th

Although it is non-toxic, normally used at high temperature, non-corrosive and cost-effective, its thermal conductivity (TC), necessary to prevent failures during instantaneous overload, is low. To enhance the TC of HTF, highly thermal conductive materials such as active carbon in lauric acid [3], carbon fibers in paraffin [4], carbon nanotubes in palmitic acid [5], exfoliated graphite in wax/LDPE [6], expanded carbon in capric-myristic acids [7], expanded graphite in palmitic acid [8], and nanographite in paraffin waxes [9] have been added to improve TC of HTF.

Among various nanomaterials with high surface area [10-18], graphene is probably the most suitable carbon based nanomaterial to increase TC of HTF due to its low thermal interface resistance associated with their 2-D planar structure [19]. The viscosity of graphene based suspension decreased at relatively high loading, whereas a monotonic increase was observed for suspensions with all the other carbon additives. Unfortunately, a single layered graphene is hard to be produced in large amount. Therefore, GO produced on the ton scale in inexpensive ways [20, 21], is potentially to be used to improve TC of materials instead.

Due to the relative ease of GO production, in this contribution, GO was added into shortening to generate naturally derived and biodegradable HTF with high TC used at high temperature for the first time. The thermal properties, thermal stability, morphology, and viscosity of the developed GOS were investigated by thermogravimetric analyser (TGA) and differential scanning calorimeter (DSC), Fourier transform infrared (FTIR), spectroscopy scanning electron microscope (SEM), and rotational viscometer, respectively.

Experimental

Materials

Graphite (< 20 μm , Sigma-Aldrich, St, Louis, Mo., USA), hydrogen peroxide (H_2O_2 , 30%, Univar, Ingleburn, Australia), potassium permanganate (KMnO_4 , Univar, Ingleburn, Australia), shortening (Crisco, Orrville, O., USA), sodium nitrate (NaNO_3 , Univar, Ingleburn, Australia), and sulfuric acid (H_2SO_4 , 98%, RCI Labscan, Bangkok, Thailand) were used as received. The deionized (DI) water was used throughout this work.

Preparation of GO and GOS

The GO particles were prepared by the modified Hummer's method [22]. In brief, graphite powder (5 g), NaNO_3 (2.5 g), and 98% H_2SO_4 (115 ml) were mixed together and stirred at 0 $^\circ\text{C}$ for 10 minute. After the slow addition of KMnO_4 (15 g), the mixture was warmed up to 35 $^\circ\text{C}$ while stirred for 30 minute. The DI water (250 ml) was gradually added. The mixture was heated at 98 $^\circ\text{C}$ for 15 minute and cooled in a water bath for 10 minute. Subsequently, DI water (700 ml) and 30% H_2O_2 (5 ml) were slowly added. After being stirred at room temperature for 30 minute and left standing for a day, the dark green precipitate was collected and washed, by decantation and centrifugation at 3,300 rpm for 30 minute, with DI water four times. The obtained GO powders were dried on a freeze dryer (Supermodulyo-230, Thermo Scientific, Waltham, Mass., USA) before mixing with melted shortening (60 $^\circ\text{C}$) at mass fractions of 1, 2, 3 or 4% w/w. The prepared GOS were then cooled down to room temperature.

Characterization of GO particles and the GOS

The morphologies of graphite, GO powders and GOS were observed under SEM (TM-1000, Hitachi, Tokyo). Their XRD patterns were recorded on X-ray diffractometer (XRD, D8 ADVANCE, Bruker, Madison, Wis., USA) operating at 40 kV and 40 mA using high power $\text{CuK}\alpha_1$ radiation with Ge-crystal (Johansson type) monochromator ($\lambda = 1.5406 \text{ \AA}$). The diffraction patterns were examined at 5-80 $^\circ$ with a scanning rate of 1 second per step and a step size

of 0.075°. The TC of the GOS (30 ml) was measured at 30, 60, and 90 °C using the transient hot-wire method [23-26], *i. e.*, the thermostat with a sensor (Thermal Logic, USA) with a diameter of 1.27 mm, a length of 60 mm, a voltage of 1.6 V and a power of 1.8 W was immersed into the samples. Each set of the experiment was conducted in triplicate. The average values and their errors were reported.

The latent heat of the samples was determined by DSC (DSC1, Mettler Toledo, Tiel, The Netherlands) from 0 to 100 °C at the heating and cooling rates of 10 °C per minute under nitrogen atmosphere. The TGA (TGA-7, PerkinElmer, Waltham, Mass., USA) was performed on a thermal analyser varying from 50 to 550 °C at a heating rate of 10 °C per minute under nitrogen atmosphere. The chemical compositions of shortening, GO powders and the GOS were characterized by FTIR (Equinox 55, Bruker, Karlsruhe, Germany). Its chemical degradation was also observed by FTIR. The viscosity of the melted GOS was measured by a rotational viscometer (VT-04F, Rion, Tokyo) with a rotor speed of 62.5 rpm and the aid of an adaptor for liquids with low viscosities at 60 °C. To assess thermal stability, the GOS with 4% w/w GO was heated up to 100 °C and cooled down to 30 °C for 100 cycles. The viscosity of the GOS was measured for every 10 cycles at 60 °C. It should be noted that each set of the viscosity measurements was conducted in triplicate. The average values and their errors were also reported.

Results and discussion

The XRD patterns of graphite and synthesized GO powders are shown in fig. 1.

The peaks at 26.6, 41.9, and 54.1° in the XRD spectrum (a) correspond to the layered structure of graphite [27]. In contrast, the spectrum (b) shows only a broad characteristic peak at 11.5°, matching with that of GO [28].

The absence of high intensity sharp peaks indicates that the layers of graphene in graphite were exfoliated. In addition, the existence of only a peak in spectrum (b) confirms the significant purity of the synthesized and purified GO powders possibly resulted from several oxygenated groups on the GO sheets [29, 30]. The morphologies of graphite, synthesized GO and the GOS with 4% w/w GO were studied under SEM and their images are shown in figs. 2(a)-2(c), respectively.

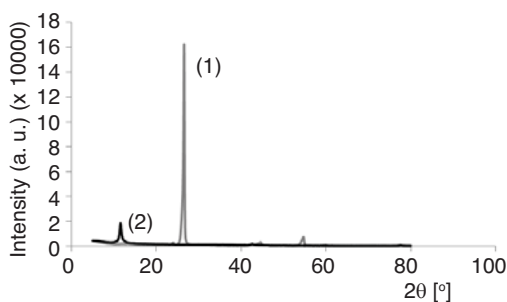


Figure 1. The XRD spectra of graphite powder (1) and GO (2)

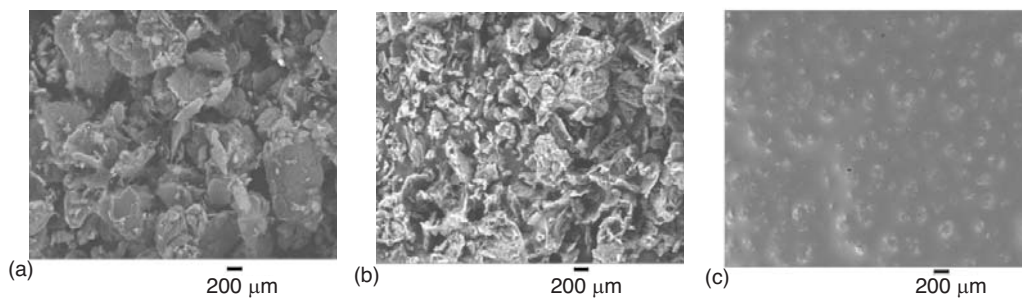


Figure 2. The SEM of (a) graphite, (b) GO and (c) GOS with 4% w/w GO

The SEM micrographs revealed that the size of graphite particles in fig. 2(a) was larger and its surface was smoother when compared to GO in fig. 2(b). This indicated that the stacks of graphene in graphite were disintegrated resulting in the increase in surface area of the resulting GO particles. Figure 2(c) reviewed that GO with an average size of $123 \pm 33 \mu\text{m}$ well dispersed in the shortening probably due to the presence of oxygen-containing functional groups on the GO surface preventing the agglomeration. This would benefit the increase in TC of the GOS which involves the collision of the particles in the materials via the convection mechanism [24]. If the particles agglomerated, the number of the particles collisions and TC of the materials would also decrease. To investigate the functional groups existed in GO and the interaction with shortening, FTIR was used for analysis of GO, shortening and the GOS. Their spectra are displayed in fig. 3.

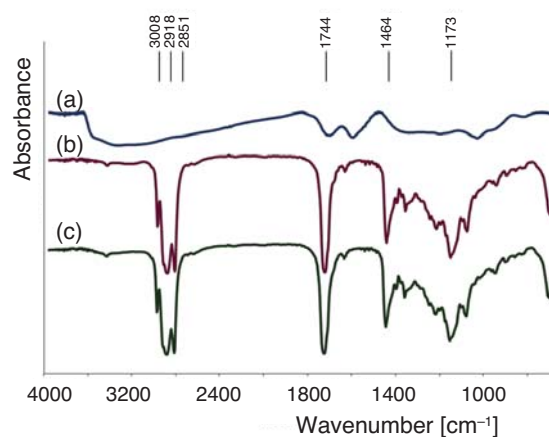


Figure 3. The FTIR spectra of (a) GO, (b) shortening, and (c) GOS with 4% w/w GO

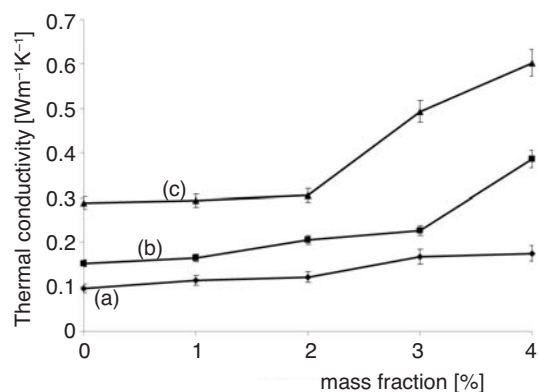


Figure 4. The TC of GOS vs. % GO mass fraction at (a) 30, (b) 60, and (c) 90 °C

Moreover, the shortening melted at ca. 47-48 °C which facilitated the movement of the added GO particles. When the numerical values of TC were considered, it was found that TC of the GOS with 4% GO was ~ 2.5 and ~ 2 times higher than that of pure shortening at 60 and 90 °C, respectively.

The spectrum (a) of GO in fig. 3 shows the three broad bands, *i. e.*, $\sim 1850 - 3600$ (carboxylic groups), ~ 1700 (C = O carboxylic acid stretching), and $\sim 1600 \text{ cm}^{-1}$ (aromatic groups) whereas the characteristic peaks at 2851, 2918, 3008 ($-\text{CH}_3$ stretching), and 1744 cm^{-1} (C = O stretching of ester groups) appear in the spectra (b) and (c) of shortening and GOS [31]. The identical infrared spectra (b) and (c) and no peak shift in the GOS spectrum could be implied that the shortening and GO were physically mixed without chemical interaction between two phases. Next, the relation between TC of the GOS and the amount of added GO at 30, 60, and 90 °C is shown in fig. 4, respectively.

Results in fig. 4 suggest that the TC of all the GOS increased with increasing the temperature and the amount of added GO. It was explained that the increase in temperature caused an increase in the number of particle collisions and, as a result, TC of the GOS [24]. However, at 30 °C, the addition of GO hardly affected the TC of GOS (a) whereas the TC of the GOS at 60 and 90 °C greatly increased with increasing the GO content from 3 to 4% and from 2 to 4%, respectively, (b) and (c). The minimum amount of the added GO particles to start the heat transfer via a collision mechanism decreased with increasing temperature. This probably resulted from the ease of GO particles collision.

It was found that the ability of GO to enhance TC of shortening was not much different from the other organic materials. For example, in 2013, TC of palmitic acid increased about three to four times after being added by GO [32]. In 2014, reduced GO, a derivative of GO, was added to polystyrene. The results showed that TC of polystyrene was enhanced by almost twice as the reduced GO concentration increased from 0 to 10% vol. [33].

Not only TC but also the viscosity of the GOS is important because it controls the ability of HTF to be flowed in pipes, which is vital in practical uses. Then, the relation between the viscosity of the GOS and the amount of GO added into the GOS at 60 °C was studied. The graph is shown in fig. 5.

It was observed that the viscosity of the GOS composites linearly increased with increasing the GO mass fraction or the volume fraction of the suspended particles [34]. Even though the TC of GOS with 4% w/w GO was higher than that of pure shortening more than twice, the viscosity of GOS, 41 mPa·s, was ca. 1.3 times of that of pure shortening, 31 mPa·s. This yielded the highly thermal conductive HTF which could be flowed easily.

The latent heat, the thermal energy released or absorbed by a material and one of the important indexes for being good HTF, of the GOS was then determined. The DSC thermograms of pure shortening and the GOS with various amounts of loaded GO powders are shown in fig. 6.

In fig. 6, the shapes and the phase change temperatures of all DSC thermograms were almost similar. The melting and the freezing temperatures of all the GOS were ca. 46 and 29 °C, respectively. This confirmed no chemical interaction between shortening and GO and no relation between the amount of added GO and the melting temperature of the GOS. To understand the change in the enthalpy of melting and freezing and the relation between the enthalpies and the amount of added GO, the latent heats of the GOS are calculated and the data are shown in tab. 1.

Table 1 reveals that the reduction in the enthalpy of melting and freezing the GOS is proportionally to the amount of loaded GO. However, there are only small differences between the enthalpies of melting and freezing of the GOS with 3% w/w GO and those with 4% w/w GO, indicating the onset of the phase separation between shortening and GO at 4% w/w GO.

To balance the homogeneity and the enhancement of the TC, the GOS with 4% w/w was chosen for the study of the thermal stability.

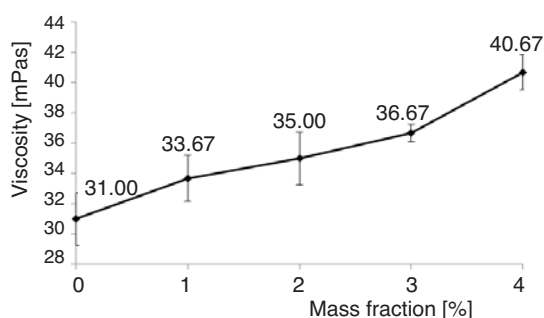


Figure 5. The viscosity of GOS as a function of % GO mass fraction

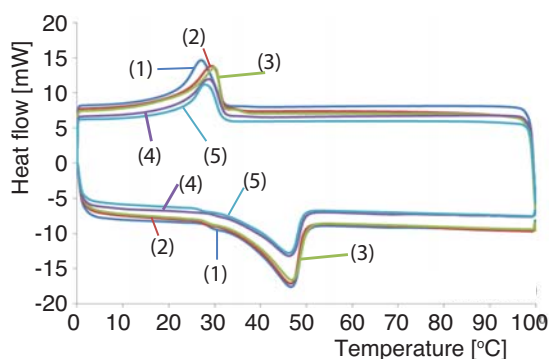
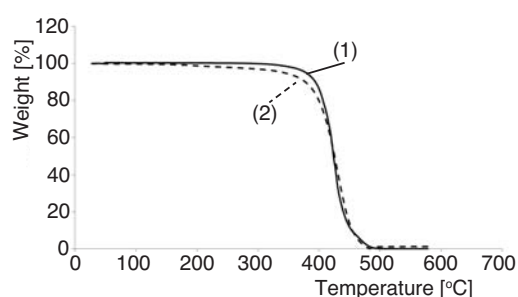
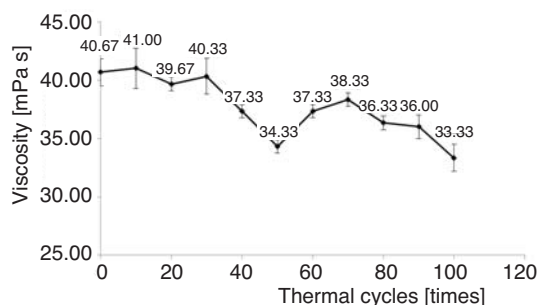


Figure 6. Differential scanning calorimetry thermograms of shortening and GOS; (1) – shortening, (2) – GOS with 1% w/w GO, (3) – GOS with 2% w/w GO, (4) GOS with 3% w/w GO, and (5) – GOS with 4% w/w GO (for color image see journal web site)

Table 1. The relation between % GO mass fraction in GOS and the enthalpy of melting and freezing and the phase change temperature of the GOS

Graphene oxide [%]	$\Delta H_{\text{melting}}$ [Jg^{-1}]	$\Delta H_{\text{freezing}}$ [Jg^{-1}]	Melting temperature [$^{\circ}\text{C}$]	Freezing temperature [$^{\circ}\text{C}$]
0	20.2	15.7	27.6	45.8
1	19.9	14.4	29.7	46.0
2	19.2	13.8	39.2	46.4
3	18.8	12.9	28.9	45.8
4	18.7	12.8	28.1	46.2

degradation of the shortening indicates the good thermal stability of the GOS and confirmed no chemical interaction between shortening and GO as formerly observed from the DSC studies [35]. To further investigate the thermal stability of the GOS with 4% w/w GO, the chemical degradation of the GOS before and after being heated and cooled for 100 cycles was examined by FTIR. It was found that the FTIR spectrum of both the freshly prepared and used GOS were identical which supports no chemical degradation and oxidation of the GOS after being heated and cooled for 100 cycles. Therefore, the GOS with 4% w/w GO could be used as HTF for at least 100 cycles. The viscosity of HTF was also measured and the results are shown in fig. 8.

**Figure 7. Thermogravimetric thermograms of shortening (1) and GOS with 4% w/w GO (2)****Figure 8. The relation between the viscosity of GOS with 4% w/w GO and the number of thermal cycles**

The viscosity of the GOS with 4% GO slightly decreased after being heated and cooled for 100 cycles because some of the long HC chains of the heated shortening were probably cut. Thus, all the results indicate the great potential of the GOS with 4% w/w GO to be used as HTF at high temperature.

Conclusions

The GOS, an environmentally friendly HTF with high TC, $0.6022 [\text{Wm}^{-1}\text{K}^{-1}]$, for being used at high temperature, was successfully prepared by mixing 4% w/w GO with a shortening. The SEM images showed that GO particles dispersed well in shortening. The DSC thermograms revealed that the latent heat of the GOS slightly decreased while their viscosity and TC increased from 31.00 to $40.67 \text{ mPa}\cdot\text{s}$ and from 0.1751 to $0.6022 [\text{Wm}^{-1}\text{K}^{-1}]$, respectively, with increasing the amount of loaded GO and temperature from 0 to 4% w/w and from 30 to 90 $^{\circ}\text{C}$, respectively.

The TGA thermograms indicated that the GOS started to be degraded at ca. 360 °C. Results from FTIR and viscometer can be implied that, after being heated and cooled at 100 °C for 100 cycles, its viscosity slightly decreased from 40.7 to 33.3 mPa·s without chemical degradation. Thus, the GOS with 4% w/w GO would be potentially used as HTF at high temperature.

Acknowledgment

Research grants from The Thailand Research Fund (TRF)/Mahidol University (TRG5680070), Mahidol University Faculty of Science and Thailand Ministry of Science and Technology to T.V., and from TRF/Commission on Higher Education to P.T. (RTA5480007) are gratefully acknowledged. The authors also express sincere thanks to Mettler Toledo (Thailand) for providing DSC facility to carry out in this research work.

References

- [1] Harris, A., et al., Measuring the Thermal Conductivity of Heat Transfer Fluids via the Modified Transient Plane Source (MTPS), *J. Therm. Anal. Calorim.*, 116 (2014), 3, pp. 1309-1314
- [2] Liu, J., et al., Thermodynamic Properties and Thermal Stability of Ionic Liquid-Based Nanofluids Containing Graphene as Advanced Heat Transfer Fluids for Medium-to-High-Temperature Applications, *Renew. Energ.*, 63 (2014), Mar., pp. 519-523
- [3] Chen, Z., et al., Synthesis and Thermal Properties of Shape-Stabilized Lauric Acid/Activated Carbon Composites as Phase Change Materials for Thermal Energy Storage, *Sol. Energ. Mat. Sol. C.*, 102 (2012), July, pp. 131-136
- [4] Elgafy, A., Lafdi, K., Effect of Carbon Nanofiber Additives on Thermal Behavior of Phase Change Materials, *Carbon*, 43 (2005), 15, pp. 3067-3074
- [5] Wang, J., et al., Increasing the Thermal Conductivity of Palmitic Acid by the Addition of Carbon Nanotubes, *Carbon*, 48 (2010), 14, pp. 3979-3986
- [6] Wang, J., et al., Enhancing Thermal Conductivity of Palmitic Acid Based Phase Change Materials with Carbon Nanotubes as Fillers, *Sol. Energ.*, 84 (2010), 2, pp. 339-344
- [7] Karaipekli, A., Sari, A., Capric-Myristic Acid/Expanded Perlite Composite as form-Stable Phase Change Material for Latent Heat Thermal Energy Storage, *Renew. Energ.*, 33 (2008), 12, pp. 2599-2605
- [8] Sari, A., Karaipekli, A., Preparation, Thermal Properties and Thermal Reliability of Palmitic Acid/Expanded Graphite Composite as form-Stable PCM for Thermal Energy Storage, *Sol. Energ. Mat. Sol. C.*, 93 (2009), 5, pp. 571-576
- [9] Li, M., A Nano-Graphite/Paraffin Phase Change Material with High Thermal Conductivity, *Appl. Energ.*, 106 (2013), June, pp. 25-30
- [10] Moghadam, A., et al., Effects of CuO/Water Nanofluid on the Efficiency of a Flat-Plate Solar Collector, *Exp. Therm. Fluid Sci.*, 58 (2014), Oct., pp. 9-14
- [11] Ho, C., et al., Thermal Performance of Al₂O₃/Water Nanofluid in a Natural Circulation Loop with a Mini-channel Heat Sink and Heat Source, *Energ. Convers. Manage.*, 87 (2014), Nov., pp. 848-858
- [12] Khaleduzzaman, S., et al., Energy and Exergy Analysis of Alumina-Water Nanofluid for an Electronic Liquid Cooling System, *Int. Commun. Heat Mass*, 57 (2014), Oct., pp. 118-127
- [13] Ho, C., Lin, Y., Turbulent Forced Convection Effectiveness of Alumina-Water Nanofluid in a Circular Tube with Elevated Inlet Fluid Temperatures: An Experimental Study, *Int. Commun. Heat Mass*, 57 (2014), Oct., pp. 247-253
- [14] Karami, N., Rahimi, M., Heat Transfer Enhancement in a PV Cell Using Boehmite Nanofluid, *Energ. Convers. Manage.*, 86 (2014), Oct., pp. 275-285
- [15] Akhavan-Behabadi, M., et al., An Empirical Study on Heat Transfer and Pressure Drop Properties of Heat Transfer Oil-Copper Oxide Nanofluid in Microfin Tubes, *Int. Commun. Heat Mass*, 57 (2014), Oct., pp. 150-156
- [16] Rimbault, B., et al., Experimental Investigation of CuO-Water Nanofluid Flow and Heat Transfer Inside a Microchannel Heat Sink, *Int. J. Therm. Sci.*, 84 (2014), Oct., pp. 275-292
- [17] Maddah, H., et al., Experimental Study of Al₂O₃/Water Nanofluid Turbulent Heat Transfer Enhancement in the Horizontal Double Pipes Fitted with Modified Twisted Tapes, *Int. J. Heat Mass Tran.*, 78 (2014), Nov., pp. 1042-1054

- [18] Naik, M., et al., Comparative Study on Thermal Performance of Twisted Tape and Wire Coil Inserts in Turbulent Flow Using CuO/Water Nanofluid, *Exp. Therm. Fluid Sci.*, 57 (2014), Sept., pp. 65-76
- [19] Yu, Z., et al., Increased Thermal Conductivity of Liquid Paraffin-Based Suspensions in the Presence of Carbon Nano-Additives of Various Sizes and Shapes, *Carbon*, 53 (2013), Mar., pp. 277-285
- [20] Mehrali, M., et al., Shape-Stabilized Phase Change Materials with High Thermal Conductivity Based on Paraffin/Graphene Oxide Composite, *Energ. Convers. Manage.*, 67 (2013), Mar., pp. 275-282
- [21] Park, S., Ruoff, R., Chemical Methods for the Production of Graphenes, *Nat. Nanotechnol.*, 4 (2009), 4, pp. 217-224
- [22] Marcano, D., et al., Improved Synthesis of Graphene Oxide, *ACS Nano*, 4 (2010), 8, pp. 4806-4814
- [23] Hakansson, B., Ross, R., Effective Thermal Conductivity of Binary Dispersed Composites over Wide Ranges of Volume Fraction, Temperature, and Pressure, *J. Appl. Phys.*, 68 (1990), 7, pp. 3285-3292
- [24] Moroe, S., et al., Thermal Conductivity Measurement of Gases by the Transient Short-Hot-Wire Method, *Exp. Heat Transfer*, 24 (2011), 2, pp. 168-178
- [25] Healy, J., et al., The Theory of the Transient Hot-Wire Method for Measuring Thermal Conductivity, *Physica B & C*, 82 (1976), 2, pp. 392-408
- [26] Alvarado, S., et al., A Hot-Wire Method Based Thermal Conductivity Measurement Apparatus for Teaching Purposes, *Eur. J. Phys.*, 33 (2012), 4, pp. 897-906
- [27] Sun, G., et al., Preparation and Characterization of Graphite Nanosheets from Detonation Technique, *Mater. Lett.*, 62 (2008), 4-5, pp. 703-706
- [28] Dmitriy, A., et al., Preparation and Characterization of Graphene Oxide Paper, *Nature*, 448 (2007), July, pp. 457-460
- [29] Park, S., et al., Colloidal Suspensions of Highly Reduced Graphene Oxide in a Wide Variety of Organic Solvents, *Nano Lett.*, 9 (2009), 4, pp. 1593-1597
- [30] Nair, R., et al., Unimpeded Permeation of Water Through Helium-Leak-Tight Graphene-Based Membranes, *Science*, 335 (2012), 6067, pp. 442-444
- [31] McMurry, J., *Organic Chemistry*, Brooks/Cole, Pacific Grove, Cal., USA, 2012
- [32] Mehrali, M., et al., Preparation and Properties of Highly Conductive Palmitic Acid/Graphene Oxide Composites as Thermal Energy Storage Materials, *Energy*, 58 (2013), Sept., pp. 628-634
- [33] Park, W., et al., Electrical and Thermal Conductivities of Reduced Graphene Oxide/Polystyrene Composites, *Appl. Phys. Lett.*, 104 (2014), 11, pp. 113101-113113
- [34] Thomas, D., Transport Characteristics of Suspension: VIII. A Note on the Viscosity of Newtonian Suspensions of Uniform Spherical Particles, *J. Colloid Sci.*, 20 (1965), 3, pp. 267-277
- [35] Fahlman, B., *Materials Chemistry*, Springer, Rotterdam, The Netherlands, 2011